In Troy McDaniel and Xueliang Liu (Eds.), Multimedia for Accessible Human Computer Interfaces, Springer, ISBN 978-3-030-70716-3, 2021.
https://doi.org/10.1007/978-3-030-70716-3_10

Enhancing Situational Awareness and Kinesthetic Assistance for Clinicians via Augmented-Reality and Haptic Shared-Control Technologies

Jay Carriere[1], Lingbo Cheng[2], and Mahdi Tavakoli[1]

[1]Department of Electrical and Computer Engineering, University of Alberta, Edmonton, Alberta, Canada
[2]College of Control Science and Engineering, Zhejiang University, Hangzhou, Zhejiang, China
jay.carriere@ualberta.ca, lingbo1@zju.edu.cn, mahdi.tavakoli@ualberta.ca

Abstract. Intraoperative situational awareness is critical for clinicians when performing complex surgeries and therapies. Augmented-reality (AR) and haptic virtual fixtures (VF) technologies can be used to increase situational awareness while still keeping the surgeon-in-the-loop. These two technologies can be used independently or together to provide various levels of assistance. 3D AR technologies provide enhanced visual feedback for the clinician, for instance, giving them the ability to "see" surgical instruments inside of tissue. Robotic assistant devices with haptic VF provide physical resistance or assistance in real-time for the clinician. Haptic VF systems can be used to enforce "no-fly zones" with varying degrees of resistance to allow the clinician to avoid damaging sensitive tissue. The assistance provided by haptic VF systems can reduce the strain on a clinician when performing a lengthy surgery, can move the surgical tool to compensate for changes in patient pose, and can increase the precision with which a clinician can perform various surgical tasks.

Keywords: Medical Robotics, Augmented Reality, Virtual Fixtures, Haptics, Assistive Technologies

1 Intraoperative Situational Awareness

Having sufficient intraoperative situational awareness is vital for physicians when performing complex procedures and therapies. Intraoperative situational awareness refers to the cognitive ability to understand where surgical tools are within the body, to determine how to manipulate the surgical tools to a desired location (or to perform a desired action), and to identify any nearby anatomical structures that should be avoided during the surgery or therapy [1]. In general, increasing a surgeon's intraoperative situational awareness will lead to an increased or successful clinical outcome of the procedure (or therapy) while reducing risks or side-effects. Using the *Perception, Planning, and Action* loop

model from robotics control theory, we can think also think of intraoperative situational awareness as consisting of: *Perception* where the surgeon must be able to sense the location of surgical tools relative to anatomical areas of interest; *Planning* where the surgeon needs to know how to move the surgical tools to a desired location. Mentally, the surgeon must continuously perform these *perception* and *planning* steps while manually performing the surgery (undertaking the *action*). This chapter will discuss the following two types of assistive technologies to increase intraoperative situational awareness, *Visual Guidance* and *Haptic Guidance*.

1.1 Visual Guidance

Visual Guidance systems display a live view of the surgical tool location and relevant anatomy. These systems enhance the vision of the surgeon, presenting them with salient information from the surgical plan and allowing them to more robustly localize surgical tools inside of tissue.

For visual guidance during surgery, the clinician can be provided with visual information on a traditional 2D TV or monitor-based display system. However, more intuitive and immersive visual feedback can be provided through an augmented reality (AR) display based on optical see-through systems. In an optical see-through AR display, computer-generated images are overlaid directly on top of the operating area and patient anatomy. They are updated in real-time to match the surgeon's viewpoint [2–4]. Sec. 3 provides an overview of visual guidance and AR systems and their application to surgical procedures.

1.2 Haptic Guidance

Haptic Guidance systems provide physical force-feedback and assistance to the clinician during the surgery. In these systems, the force feedback is provided by a robot end-effector holding the surgical tool (or the end-effector itself is a surgical tool) to the clinician or from a surgical console (in a system like the da Vinci surgical robot).

For haptic guidance, a compliant robot controller is designed to use active constraints/virtual fixtures to provide the assistive and resistive force to the clinician. These virtual fixtures (VF) can be used to enforce rigid "no-fly" zones during the surgery, provide resistance near sensitive anatomical areas, or can provide assistance to the surgeon by helping to move the surgical tool to a desired position/location (with respect to the surgical plan) or follow anatomical motion [5]. Utilizing VF within the robot control loop allows for intuitive hands-on human/robot collaboration while still providing substantial force assistance/resistance to the clinician in a safe and stable manner [6]. Sec. 4 will discuss the use of virtual fixtures for haptic guidance in surgery.

1.3 Applications of Visual and Haptic Guidance in Surgery

As motivation for the visual and haptic guidance technologies discussed in this chapter, Sec. 2 will provide some background information on two surgical pro-

cedures used in the treatment and diagnosis of cancer, *percutaneous biopsy* and *mandible reconstruction*. Percutaneous (needle-based) biopsies are popular for extracting suspect tissue as part of confirming a cancer diagnosis. These needle-based biopsies are commonly performed as they are cost-effective, minimally invasive, low risk, and fast. One complication of needle-based biopsies is that the procedure's diagnostic efficacy and accuracy depend on the accuracy with which the biopsy needle is inserted into the target tissue. Mandible reconstruction is done to surgically repair or replace portions of the lower jaw bone, which have been damaged due to cancerous growths. A donor bone, typically a portion of the fibula from the patient, is used for reconstructing the jaw bone. The fibula portion is then cut into a number of precise segments. These segments are cut to different sizes and with different angles so that when they are assembled together, much like a 3D jigsaw puzzle, they will match the shape and curvature of the existing jaw bone. The success of the mandible reconstruction depends on the accuracy with which the fibula segments are cut.

This chapter will also provide an overview of practical visual and haptic guidance assistive systems to increase intraoperative awareness for biopsy and lower mandible reconstruction in Sec. 5, from our previously published works in [7] and [8] respectively.

2 Background

Oncology, dealing with the diagnosis and treatment of cancers, is a particularly complex field of medicine where diagnostic accuracy and treatment efficacy are paramount. Given the substantial number of different types of cancers, with varying degrees of severity (even within the same type of cancer), most surgical oncology procedures are either pre-planned using medical image guidance (preoperative imaging) and/or utilize real-time medical image feedback (intraoperative imaging) during the procedure [9]. This chapter will discuss assistive technologies that can be used to increase intraoperative situational awareness for clinicians during surgical oncology procedures, which capitalize on this available medical image planning/feedback. These assistive technologies help reduce the cognitive load on physicians by providing them with enhanced (visual and physical) *perception* to more accurately and effectively follow a desired surgical plan.

The surgical assistant systems described within this chapter will be discussed using two different surgical oncology procedures, biopsy and mandible reconstruction (fibula osteotomy), to provide practical examples of their utility. The assistance systems are designed to provide information (guidance) based on preoperative and intraoperative medical images used for these procedures. In general, there are numerous medical imaging modalities that can be used to detect cancerous cells, develop surgical plans, and monitor surgical progress [9]. For biopsy or percutaneous procedure guidance, the most commonly used imaging modalities are x-ray (CT or Mammogram), ultrasound (US), MRI, and optical imaging [10]. In the planning of the fibula osteotomy portion of mandibular

reconstruction surgery, to be discussed below, x-ray (standard 2D and CT) images are the primary imaging modality [11–13]. Therefore, both the visual and haptic guidance technologies can theoretically provide similar benefits to other image-guided semi-autonomous surgical systems.

2.1 Biopsy

Percutaneous, or core needle, biopsy is a common procedure to collect tissue samples from suspected cancerous tissue within the body. In percutaneous biopsy, a biopsy needle is inserted through the skin and guided into the tissue to be sampled. Once the biopsy needle has been correctly positioned a small sample of tissue is extracted using a cutting head on the tip of the needle. Core needle biopsies are generally preferred over surgical biopsies as they are faster, easier to perform, have minimal cosmetic effect, and are less invasive for the patient [14, 15]. For accurate diagnosis, the correct placement of the biopsy needle tip is critical and often intraoperative US, MRI, and x-ray (mammogram) images are used to help guide the clinician during needle insertion [14].

A number of retrospective studies have shown that, even with image guidance, roughly $2.2\% - 3.5\%$ of core needle biopsies result in false negatives [16, 17]. The primary reason for these false negative tests is the result of improperly placing the needle with respect to the desired target tissue. The placement inaccuracy is primarily caused by poor visualization and localization of the needle tip and target tissue in the intraoperative images [16, 18]. While MRI is an ideal imaging modality for accurate localization of the needle with superior soft-tissue contrast capability, MRI imaging is time consuming, expensive, and not universally available. Therefore, US imaging is the preferred imaging modality for most core needle biopsy procedures, and has been shown to result in more accurate needle placement than x-ray mammography [16]. There are limitations to US image guidance, in that current clinical US machines tend to be low resolution, noisy, and only provide moderate soft tissue contrast.

Percutaneous biopsy, therefore, provides an ideal example of a procedure that can be assisted through the use of enhanced visual guidance. A brief summary of the experimental setup for visual guidance, from [7], will be presented in Sec. 5 where the amount of assistance provided by visual guidance technologies in both the 2D monitor-based display and the AR display modalities was compared; shown in Figs. 1b and 1a respectively.

2.2 Mandible Reconstruction

A mandibulectomy may be performed if a tumor threatens or invades the mandible (lower jaw bone) of a patient. If the tumour is small, or well confined to a specific area, the tumour and a minimal portion of the impacted jaw bone will be removed (marginal mandibulectomy). For more aggressive or widespread cancers, where a marginal mandibulectomy would be ineffective, it is necessary to remove the entire mandible and the tumor tissue surrounding it in a procedure known as segmental mandibulectomy.

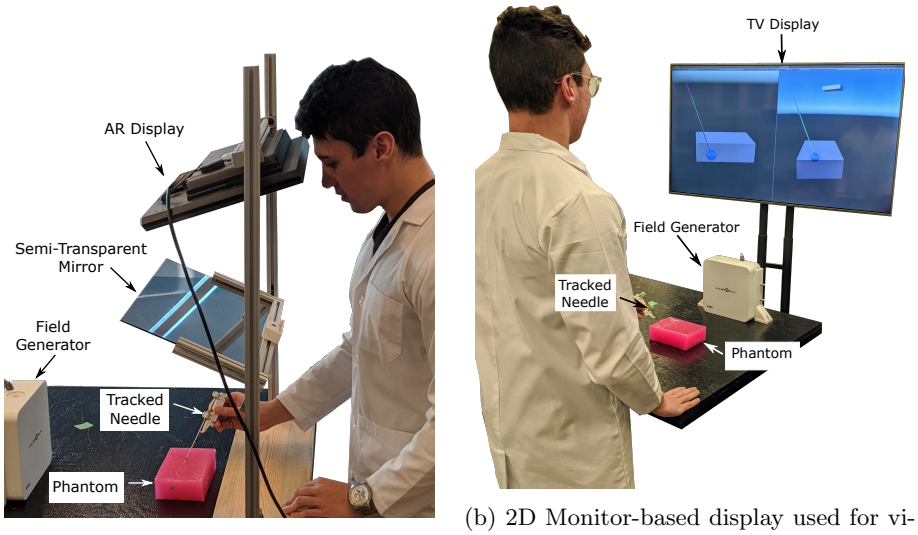

(a) Augmented-reality display used for visual guidance during the biopsy experiments.

(b) 2D Monitor-based display used for visual guidance during the biopsy experiments, showing a front and side view of the surgical scene.

Fig. 1: The two different display methods, AR and monitor-based, used for visual guidance during biopsy experiments. Both displays show current needle position, desired needle trajectory, and target phantom tumour.

After segmental mandibulectomy, the lower jaw bone must be surgically recreated through a procedure known as mandibular reconstruction. There has been a great deal of interest and significant progress in mandibular reconstruction over the last 50 years [19–21]. An autograft bone coming from the patient, and surrounding soft/vascular tissue, is used to recreate the mandible. Fibula free-flap reconstruction, utilizing a portion of the fibula and calf tissue, is the most widely used autograft source [11–13]. After removal, the fibula has to be cut down into a number of precisely shaped pieces (fibula osteotomy) that are bonded together to recreate the shape and curve of the removed jaw bone. Using CT and x-ray images, virtual surgical planning is used to develop the cutting plan for fibula osteotomy to maximize the esthetic and functional outcomes of the reconstructed mandible. Fibula osteotomy is a highly challenging surgical procedure, where there may be compound angles between the desired cutting planes on either side of each cut fibula piece. Any deviation from the virtual plan and the shapes of the fibula pieces after cutting will impact the resulting esthetic and functional outcomes of the reconstructed mandible, and can increase the risk of rejection and severe side-effects [11–13].

Due to these risks, in conventional mandibular reconstruction, fabrication and use of patient-specific cutting guides/templates is used to minimize the

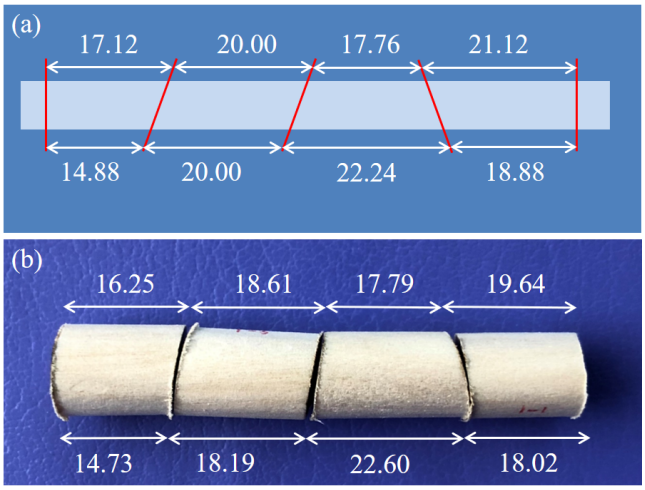

Fig. 2: (a) Desired fibula segments from the front view. (b) Measured results of fibula segments implemented by using guidance with AR and VF from the front view, units are in mm.

deviation between the surgical plan and the resultant cut fibula segments. These templates, along with rapid prototyped models of the patient's jaw and fibula bones, has led to significant improvements in mandible reconstruction [22–25]. The fabricated cutting guide/templates significantly improve the accuracy with which fibula free flap osteotomy can be done [26, 27], however, they have some significant limitations. Due to precision, strength, and sterility requirements for the cutting guide/templates, they are expensive, time-consuming to produce, and extremely difficult to modify after fabrication.

As a more flexible and dynamic alternative to the fabricated cutting guide/templates, an alternative is to use a (non-robotic) image-guided navigation system when cutting the fibula based on the initial surgical plan [28]. In these systems, the surgeon is guided by the pre-planned cutting planes/locations, which are projected onto the skeletal anatomy. While these image-guided systems provide clinical benefits by allowing more freedom during preoperative planning and allow for modifying the plan intraoperatively, it is extremely difficult for a surgeon to match the position and orientation of the projected cutting planes with the required precision, as shown in Fig. 2. To compensate for this, surgical robotic and image-guided robotic systems have been developed for fibula extraction and cutting. These systems have shown significant advances in terms of planning flexibility, time and cost savings, and cutting precision with respect to the conventional template or non-robotic image-guided approaches [29–31].

Given the existing research on image-guided robotic and non-robotic systems for fibula osteotomy, it is clear that the precision and accuracy required during fibula osteotomy provides an ideal surgical procedure with which to evaluate

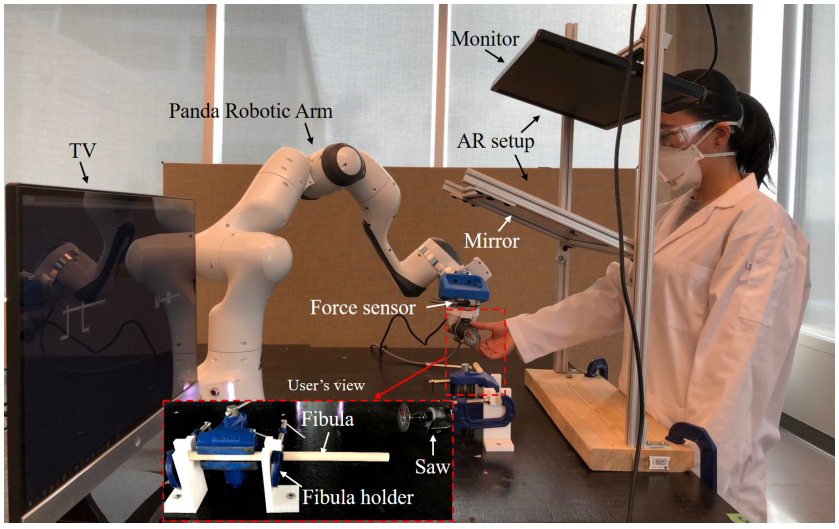

Fig. 3: Experimental setup for fibula osteotomies: robot, force sensor, saw, simulated fibula bone, fibula holder, TV screen, and AR setup.

visual guidance and haptic guidance assistant systems. A brief description of the experimental setup used in [8] for visual and haptic guidance are given in Sec. 5, and are shown in Fig. 3.

3 Visual Guidance Technologies

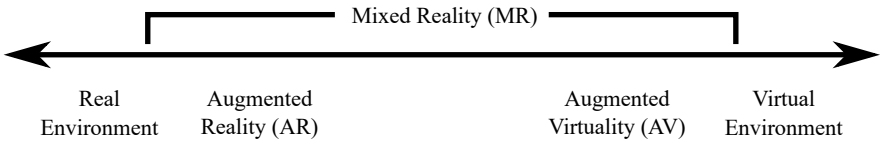

Fig. 4: The Virtuality Continuum introduced by [32] to categorize different mixed reality environments.

Visual guidance can be provided by a surgical assistance system through a number of display modalities. The two modalities we will discuss within this chapter are monitor-based 2D displays and AR displays. Here it is important to note that standard 2D monitor, TV, or smartphone displays can be used as components when creating video-see-through (VST) and optical-see-through (OST) AR displays. The distinction between what we refer to as a 2D display and AR display is based on the Virtuality Continuum, which was proposed by [32]; see Fig. 4. As will be discussed in Sec. 3.1, the key difference between a

2D display and an AR display is that AR technology utilize perspective, scaling, and pose information to display virtual objects such that they appear to co-exist with (or are overlaid on top of) real-world objects from the observer's viewpoint. Within the Virtuality Continuum in Fig. 4, augmented reality is shown as being more akin to the real-world than virtual reality. When we refer to 2D displays, we are referring to simple rendering/display technologies which show virtual objects with a perspective or scale independent from real-world objects. Our definition of 2D displays then corresponds to the virtual environment shown in Fig. 4.

3.1 Augmented Reality Display

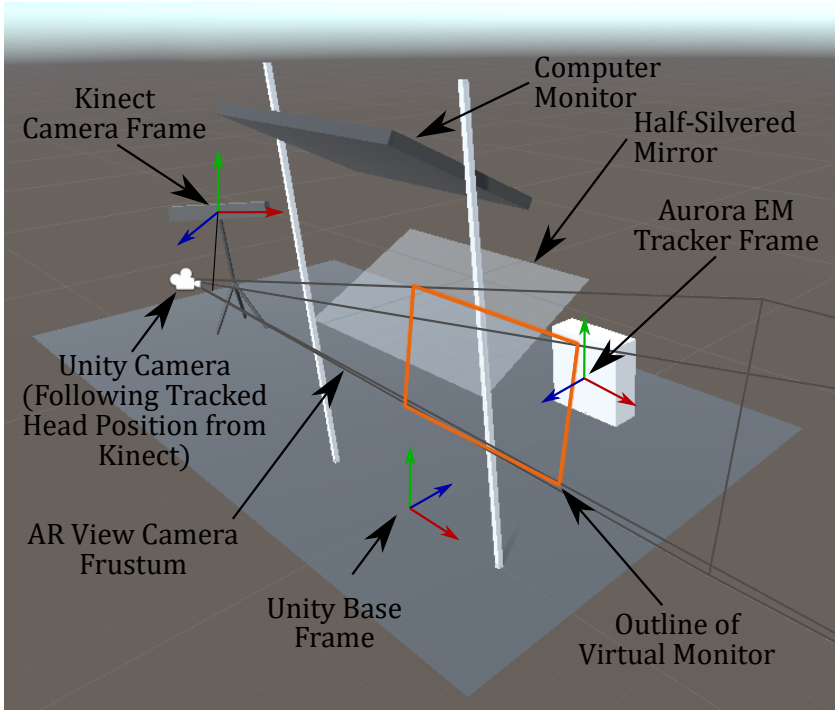

Fig. 5: For the AR display system, a scale-accurate copy of the physical setup was modelled within Unity for the biopsy and fibula osteotomy experiments. The position of the Unity camera is updated in real-time to follow the user's head motion to ensure that the overlaid projection of objects rendered from the virtual-world surgical scene matches their real-world counterparts.

AR is defined as a technology that projects (or overlays) virtual objects onto real-world objects. The key feature of AR displays is that there is a continuously updated mapping between the viewpoint of the observer, real-world locations

and objects, and the locations of virtual objects. This mapping allows for the motion of virtual objects to seamlessly match those of real-world objects with respect to the observer's viewpoint. The use of AR technologies during surgical interventions has been and continues to be an active area of research [2–4]. Advances in medical image and 3D graphic processing technologies have allowed for AR systems to be adapted to a growing number of surgical applications, including general open surgeries [2], laparoscopic oncology surgeries [33], and orthopedic surgeries [4]. The real-time 3D rendered graphics, and image overlaying, used in immersive AR displays can be implemented using any number of available general-purpose 3D graphics rendering libraries/toolkits, such as Unity (Unity Technologies, San Francisco, CA, USA), or with specialized toolkits for medical image display and analysis such as 3D Slicer [34].

Depending on the application area, there are a number of possible ways that AR displays can work to project virtual objects onto real-world objects. For instance, video-see-through displays are a common AR display method where virtual objects are superimposed on top of real-world objects captured in a live video stream. This projection style is commonly used for AR videogames, for example, Pokemon Go (Niantic Inc., San Francisco, CA, USA), as it can be easily implemented using the built-in camera and screen in smartphones and tablets. This style of AR display has also been used for prototype and research medical AR systems, with some using smartphones or tablets, or to overlay virtual objects onto a video stream captured by an endoscopic or laparoscopic camera during surgery [3, 33].

The AR display used in this work is an optical-see-through system, where the user can see the simulated surgical scene through a semi-transparent (half-silvered) mirror [35, 36, 7, 8]. The rendered images for the AR display are output to a monitor, which are then reflected on the half-silvered mirror to blend with the user's view of the surgical scene. This allows any salient surgical tool or anatomical information to be placed correctly on top of real-world reference objects in the surgical scene when presented to the user, giving them an x-ray-like ability to see things inside of tissue (or any other real-world object). The mirror and monitor are mounted at an appropriate distance above the surgical workspace to ensure an adequate amount of free workspace for the user to manipulate surgical tools, when performing the simulated surgical procedure. One major advantage of optical-see-through displays, like this one, is that they offer an additional safety factor over video-see-through AR displays. Even if the screen or display device fails, it is still transparent and therefore, will not abruptly obstruct the view of a clinician during surgery.

The half-silvered mirror AR display can be mounted either rigidly or with a swivel joint, such that it can be rotated out of the way, in front of the surgical scene. While head-mounted optical-see-through devices, such as the Microsoft HoloLens and HoloLens2 (Microsoft, Redmond, WA), are commercially available, they have been found to be generally unsuitable for use within surgical settings due to cost, complexity, weight, and optical limitations, making it difficult to focus on both real-world and virtual content simultaneously [37, 38]. The semi-

transparent mirror optical-see-through AR display is both low-cost and does not suffer from the same optical limitations as a head-mounted optical-see-through [36, 7, 8]; see Fig. 1a.

With a single monitor being reflected by the semi-transparent mirror, the AR display is able to provide a single-view camera/viewpoint perspective. To provide an immersive display for the user, the user's head is tracked in 3D, using a Kinect v2 depth camera, and the position of the rendering camera in Unity (see Fig. 5) is updated to follow the user's head in 3D. Being as the system provides only a single-view camera rendering, the 3D position of the user's two eyes are tracked and the desired position for the Unity camera is calculated to be centered between them (roughly corresponding to the bridge of the user's nose). With this live head tracking, the Unity camera view of the surgical scene matches the user's view and perspective, which not only allows the virtual objects to be overlaid correctly but also provides parallax (depth-cue) information. The effect of these parallax depth-cues is that as users move their head around they are able to see different sides of the virtual objects (which are mapped appropriately to match the user's viewing angle). Due to how the human visual system processes and retains visual information, these depth cues are stored and processed such that the user perceives a rich 3D environment which is a phenomena known as motion parallax [39]. With the head-tracking and depth-cue information, the AR display is able to provide immersive AR information, overlaid onto the surgical scene, in a low-cost and highly-configurable platform.

When looking at the surgical scene, the user sees a reflection of the 2D monitor in the semi-transparent mirror. The reflected monitor, referred to as the "virtual monitor", appears to be hovering in space between the back-side of the mirror and the surgical scene; see Fig 6. The location of the virtual monitor is dependent on the relative distances and angles between the physical monitor and the mirror. By measuring these angles and offsets, using landmarks on the AR setup, the location of the corners of the virtual monitor can be calculated. By using a generalized perspective projection [40], the view frustum of the Unity camera can be constrained to correspond exactly with the corners of the virtual monitor (as if the user is looking through a virtual window); a full explanation of the projection calibration is given in [7]. The parameters of the perspective projection matrix are designed such that the AR images are automatically flipped (during rendering), to provide a correct view when reflected in the mirror; ensuring the rendered virtual objects match the position, scale, and orientation of real-world objects from the user's viewpoint. Fig. 5 shows the corners of the virtual monitor, and the constrained view frustum of the Unity camera, as a result of the generalized perspective projection calculations.

3.2 Monitor-based 2D Display

For 2D visual guidance during surgery, the system displays two 2D images, top and front views of the surgical scene and shows the current pose of the surgical tool, the biopsy needle or saw. As with the AR display system, the virtual surgical scene was modelled and rendered using Unity. The 2D display provides

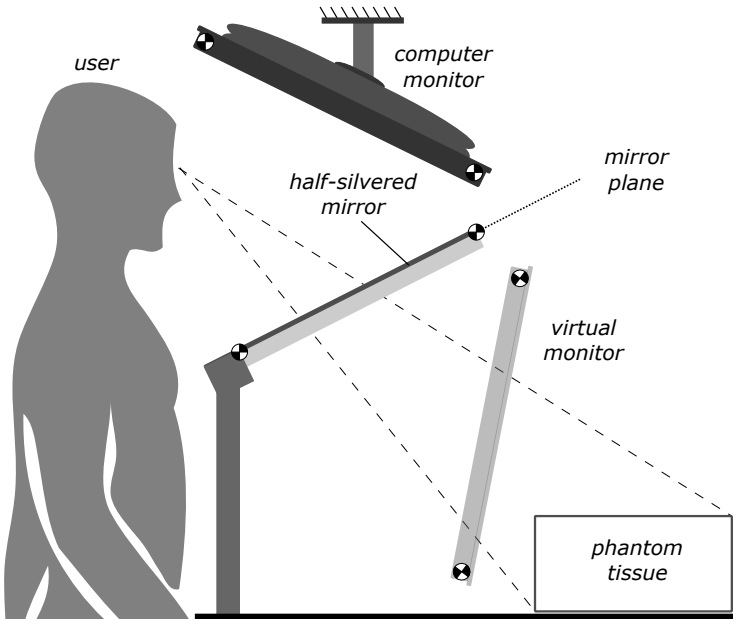

Fig. 6: Diagram of the single-camera AR setup for the biopsy experiment. The "virtual-monitor" is the reflected image of the physical monitor in the semi-transparent mirror.

salient surgical guidance information through projections of the desired biopsy target or the fibula cutting planes in both views. Thus, this image-guided surgery task provides visual guidance comparable to conventional surgical tool tracking, wherein a live image of the surgical tool is overlaid on top of CT or x-ray patient images. For visualization, a standard computer monitor was placed near physical simulated surgical setups and showed real-time surgical performance by displaying desired and actual tool (saw or biopsy needle) positions and orientations. During the simulated surgical procedures using the 2D-only visual guidance assistance in [7] and [8], the goal was for the operator to orient the surgical tool to match the desired tool pose shown on the display.

4 Haptic Guidance

The level of assistance provided during surgery by a robotic surgical system can be defined in terms of six discrete levels of automation [41, 42]. At *Level 0*, the first level of automation, the robotic or surgical system is under the clinician's direct control and no assistance is provided (i.e. fully manual surgery). At *Level 5*, the highest level of automation, the robotic surgical system is fully automatic and requires no input or control from the clinician. Given the inherent complexity and safety issues associated with high levels of automation,

most research within the literature is focused on providing unobtrusive surgical assistance with the *surgeon-in-the-loop*, where the robotic system is working in collaboration with the surgeon while they are performing most aspects (or all) of the surgery manually.

Haptic guidance force-feedback during surgery can be provided to a clinician, or a user controlling a robot, through a force-feedback capable control console in a dual-robot teleoperated system, or directly to the clinician holding on to a surgical tool which is connected to the end-effector of a single-robot collaborative system. In either single-robot or dual-robot teleoperated systems, haptic fixtures can be used to model and implement resistive and assistive force fields in free space [5]. For human-robot cooperation, virtual fixtures provide an excellent balance between full autonomy and direct human control [6]. Haptic guidance during the fibula osteotomy surgical simulation was provided by a single Panda collaborative robot; see Fig. 3. An admittance controller was used to render the effect of the haptic fixtures while ensuring the robotic system remained compliant. Within the level of automation frameworks outlined in [41, 42], the admittance control and virtual fixture technologies for increasing situational awareness are part of *Level 1* of automation, providing enhanced perception and/or guidance to the surgeon.

4.1 Admittance Control

Admittance control is a common control methodology used to allow for hands-on direct co-manipulation of a surgical tool attached to the end-effector of a robotic system [43]. The admittance controller was utilized to allow for the operator to collaborate with the surgical robot assistant smoothly and to minimize the operator's hand tremor and the vibration caused by the surgical saw [44–50]. The admittance controller ensures that the surgical robot is compliant while still providing appreciable haptic guidance to the user.

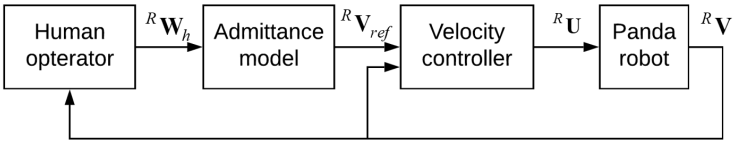

Fig. 7: Admittance controller for the robot.

The controller design is outlined in Fig. 7. Here, ${}^{R}\mathbf{W}_h$ is the interaction force-torque (wrench) between the robot end-effector and the operator, which is measured directly through a 6-DOF force sensor, as expressed in the frame $\{R\}$. The pre-programmed admittance model receives inputs, ${}^{R}\mathbf{W}_h$, and generates reference Cartesian (both translational and angular) velocity for the robot,

${}^{R}\mathbf{V}_{ref}$, to track. As the saw is mounted on the robot end-effector, we use the position and orientation of the robot end-effector to indicate the position and orientation of the saw blade for the sake of brevity. A velocity controller is used for the robot and outputs control signals, ${}^{R}\mathbf{U}$, to the robot. The actual Cartesian velocity of the robot end-effector is denoted as ${}^{R}\mathbf{V}$.

The desired admittance model in this study is designed as

$$\mathbf{M}\,{}^{R}\mathbf{V}_{ref} + \mathbf{C}\,{}^{R}\mathbf{V}_{ref} = k_f\,{}^{R}\mathbf{W}_h \tag{1}$$

where $\mathbf{C}$ and $\mathbf{M}$ are the virtual damping and inertia (6-by-6 diagonal) matrices of the admittance model given in [8]. In order to avoid restoring forces in free-space, the stiffness term is set to be zero matrix. Also, k_f is a force scaling factor.

5 Experimental Setup for Demonstration Assistive Systems

The experimental setups (shown in Figs. 1a, 1b, and 2) for the demonstration assistive systems, in [7, 8], contain some equipment in common. The virtual surgical objects and scenes for 2D and AR displays used in both setups for visual guidance were rendered using the Unity Engine (Version 2019.2.21 Unity Technologies, San Francisco, CA, USA). The calculations of the AR display projective parameters and experimental data analysis were done in MATLAB/Simulink R2019a (The MathWorks Inc, Natwick, MA, USA).

5.1 Experimental Percutaneous Biopsy Setup

For the percutaneous biopsy task, phantom tumours were fabricated and embedded into a rectangular opaque tissue phantom. Super soft plastisol (M-F Manufacturing Company, Fort Worth, Texas, USA), which is similar in characteristics to biological tissue, was used to create the tumour and phantom tissue. The plastisol phantom tumours, located inside the tissue phantom, have the same material properties as the surrounding tissue and are sized to approximate tumors seen clinically. Using the same plastisol for the phantom tissue and tumour replicates the characteristics of a non-palpable tumour. To track the location of the biopsy needles in real-time an electromagnetic tracker, the NDI Aurora V2 System (NDI Medical, Waterloo, Ontario, Canada), was used. The biopsy needle and tissue phantom were instrumented with 6-DOF sensors (NDI Item ID 610029) to track the position and orientation of the needles and tumour. The needle tracking information was used to update the position of the biopsy needle for both the 2D and AR display modality experiments.

5.2 Experimental Fibula Osteotomy Setup

For haptic guidance in the fibula osteotomy study, a Panda Robotic Arm (Franka Emika GmbH, Munich, Germany) equipped with an Axia80-M20 force/torque

sensor (ATI Industrial Automation, Inc., Apex, NC, USA) was used as the surgical robot (Fig. 2). A rotary saw (Dremel 4300-5/40, Toluca, Mexico) was attached to the robot end-effector to act as a proxy for a surgical bone saw used in fibula osteotomy. The feasibility of the proposed methods is verified through proof-of-concept experimentation by performing fibula osteotomies on several simulated fibula bones which are wood dowels with a diameter of half an inch. Although the stiffnesses of the wood dowel and the fibula bone are slightly different, both are rigid objects, and both are designed to effectively cut through them. Therefore the difference in material properties has a trivial and negligible effect on the experimental results. The admittance controller for the virtual fixtures was implemented using MATLAB/Simulink R2019a, on a PC running Ubuntu 16.04 LTS, containing an Intel Core i5-8400 running at 4.00 GHz (Intel Corporation, Santa Clara, CA, USA).

References

1. I. N. Nomikos, "Situational awareness in surgery," *Hellenic Journal of Surgery*, vol. 90, no. 6, pp. 282–284, 2018. [Online]. Available: https://doi.org/10.1007/s13126-018-0490-y
2. B. Fida, F. Cutolo, G. di Franco, M. Ferrari, and V. Ferrari, "Augmented reality in open surgery," *Updates in Surgery*, vol. 70, no. 3, pp. 389–400, 2018. [Online]. Available: https://doi.org/10.1007/s13304-018-0567-8
3. M. Eckert, J. S. Volmerg, and C. M. Friedrich, "Augmented reality in medicine: Systematic and bibliographic review," *JMIR Mhealth Uhealth*, vol. 7, no. 4, p. e10967, Apr 2019. [Online]. Available: http://mhealth.jmir.org/2019/4/e10967/
4. L. Jud, J. Fotouhi, O. Andronic, A. Aichmair, G. Osgood, N. Navab, and M. Farshad, "Applicability of augmented reality in orthopedic surgery - a systematic review," *BMC Musculoskeletal Disorders*, vol. 21, no. 1, p. 103, 2020. [Online]. Available: https://doi.org/10.1186/s12891-020-3110-2
5. S. A. Bowyer, B. L. Davies, and F. Rodriguez y Baena, "Active constraints/virtual fixtures: A survey," *IEEE Transactions on Robotics*, vol. 30, no. 1, pp. 138–157, 2014.
6. J. J. Abbott, P. Marayong, and A. M. Okamura, "Haptic virtual fixtures for robot-assisted manipulation," in *Robotics Research*, S. Thrun, R. Brooks, and H. Durrant-Whyte, Eds. Berlin, Heidelberg: Springer Berlin Heidelberg, 2007, pp. 49–64.
7. D. Asgar-Deen, J. Carriere, E. Wiebe, L. Peiris, A. Duha, and M. Tavakoli, "Augmented reality guided needle biopsy of soft tissue: A pilot study," *Frontiers in Robotics and AI*, vol. 7, p. 72, 2020. [Online]. Available: https://www.frontiersin.org/article/10.3389/frobt.2020.00072
8. L. Cheng, J. Carriere, J. Piwowarczyk, D. Alto, N. Zemiti, M. de Boutray, and M. Tavakoli, "Admittance-controlled robotic assistant for fibula osteotomies in mandible reconstruction surgery," *Advanced Intelligent Systems*, 2020.
9. J. V. Frangioni, "New technologies for human cancer imaging," *Journal of clinical oncology*, vol. 26, no. 24, p. 4012, 2008.
10. C. Rossa and M. Tavakoli, "Issues in closed-loop needle steering," *Control Engineering Practice*, vol. 62, pp. 55 – 69, 2017. [Online]. Available: http://www.sciencedirect.com/science/article/pii/S0967066117300606

11. D. A. Hidalgo, "Fibula free flap: A new method of mandible reconstruction," *Plastic and Reconstructive Surgery*, vol. 84, no. 1, 1989. [Online]. Available: https://journals.lww.com/plasreconsurg/Fulltext/1989/07000/Fibula_Free_Flap__A_New_Method_of_Mandible.14.aspx
12. D. A. Hidalgo and A. L. Pusic, "Free-flap mandibular reconstruction: a 10-year follow-up study." *Plastic and reconstructive surgery*, vol. 110, pp. 438–49; discussion 450–1, Aug 2002.
13. E. I. Chang, M. P. Jenkins, S. A. Patel, and N. S. Topham, "Long-term operative outcomes of preoperative computed tomography-guided virtual surgical planning for osteocutaneous free flap mandible reconstruction." *Plastic and reconstructive surgery*, vol. 137, pp. 619–23, Feb 2016.
14. L. Liberman, "Percutaneous imaging-guided core breast biopsy: state of the art at the millennium," *American Journal of Roentgenology*, vol. 174, no. 5, pp. 1191–1199, 2000.
15. S. H. Parker, F. Burbank, R. J. Jackman, C. J. Aucreman, G. Cardenosa, T. M. Cink, J. L. Coscia Jr, G. Eklund, W. Evans 3rd, and P. R. Garver, "Percutaneous large-core breast biopsy: a multi-institutional study." *Radiology*, vol. 193, no. 2, pp. 359–364, 1994.
16. M. Boba, U. Kołtun, B. Bobek-Billewicz, E. Chmielik, B. Eksner, and T. Olejnik, "False-negative results of breast core needle biopsies–retrospective analysis of 988 biopsies," *Polish journal of radiology*, vol. 76, no. 1, p. 25, 2011.
17. L. Liberman, D. D. Dershaw, J. R. Glassman, A. F. Abramson, E. A. Morris, L. R. LaTrenta, and P. P. Rosen, "Analysis of cancers not diagnosed at stereotactic core breast biopsy." *Radiology*, vol. 203, no. 1, pp. 151–157, 1997.
18. J. H. Youk, E.-K. Kim, M. J. Kim, J. Y. Lee, and K. K. Oh, "Missed breast cancers at us-guided core needle biopsy: how to reduce them," *Radiographics*, vol. 27, no. 1, pp. 79–94, 2007.
19. A. Castermans, A. van Garsse, and R. Vanwijck, "Primary reconstruction of the mandible after resection for oral cancer." *Acta chirurgica Belgica*, vol. 76, pp. 203–8, Mar-Apr 1977.
20. H. O. Defries, "Reconstruction of the mandible: Use of combined homologous mandible and autologous bone," *Otolaryngology–Head and Neck Surgery*, vol. 89, no. 4, pp. 694–697, 1981, pMID: 6793984. [Online]. Available: https://doi.org/10.1177/019459988108900433
21. R. A. Lowlicht, M. D. Delacure, and C. T. Sasaki, "Allogeneic (homograft) reconstruction of the mandible." *The Laryngoscope*, vol. 100, pp. 837–43, Aug 1990.
22. Y.-f. Liu, L.-w. Xu, H.-y. Zhu, and S. S.-Y. Liu, "Technical procedures for template-guided surgery for mandibular reconstruction based on digital design and manufacturing." *Biomedical engineering online*, vol. 13, p. 63, May 2014.
23. E. Matros, E. Santamaria, and P. G. Cordeiro, "Standardized templates for shaping the fibula free flap in mandible reconstruction." *Journal of reconstructive microsurgery*, vol. 29, pp. 619–22, Nov 2013.
24. K. A. Rodby, S. Turin, R. J. Jacobs, J. F. Cruz, V. J. Hassid, A. Kolokythas, and A. K. Antony, "Advances in oncologic head and neck reconstruction: systematic review and future considerations of virtual surgical planning and computer aided design/computer aided modeling." *Journal of plastic, reconstructive & aesthetic surgery : JPRAS*, vol. 67, pp. 1171–85, Sep 2014.
25. R. Sieira Gil, A. M. Roig, C. A. Obispo, A. Morla, C. M. Pagès, and J. L. Perez, "Surgical planning and microvascular reconstruction of the mandible with a fibular flap using computer-aided design, rapid prototype modelling, and precontoured

titanium reconstruction plates: a prospective study." *The British journal of oral & maxillofacial surgery*, vol. 53, pp. 49–53, Jan 2015.

26. H. Logan, J. Wolfaardt, P. Boulanger, B. Hodgetts, and H. Seikaly, "Exploratory benchtop study evaluating the use of surgical design and simulation in fibula free flap mandibular reconstruction." *Journal of otolaryngology - head & neck surgery = Le Journal d'oto-rhino-laryngologie et de chirurgie cervico-faciale*, vol. 42, p. 42, Jun 2013.
27. G. Papadopoulos-Nydam, J. Wolfaardt, H. Seikaly, D. O'Connell, J. Harris, M. Osswald, S. Nayar, and J. Rieger, "Comparison of speech and resonance outcomes across three methods of treatment for maxillary defects," *International Journal of Maxillofacial Prosthetics*, vol. 1, pp. 2–8, 2017.
28. W. M. Rozen, J. W. C. Ting, M. Leung, T. Wu, D. Ying, and J. Leong, "Advancing image-guided surgery in microvascular mandibular reconstruction: combining bony and vascular imaging with computed tomography-guided stereolithographic bone modeling." *Plastic and reconstructive surgery*, vol. 130, pp. 227e–229e, Jul 2012.
29. A. H. Chao, K. Weimer, J. Raczkowsky, Y. Zhang, M. Kunze, D. Cody, J. C. Selber, M. M. Hanasono, and R. J. Skoracki, "Pre-programmed robotic osteotomies for fibula free flap mandible reconstruction: A preclinical investigation." *Microsurgery*, vol. 36, pp. 246–9, Mar 2016.
30. X. Kong, X. Duan, and Y. Wang, "An integrated system for planning, navigation and robotic assistance for mandible reconstruction surgery," *Intelligent Service Robotics*, vol. 9, no. 2, pp. 113–121, 2016. [Online]. Available: https://doi.org/10.1007/s11370-015-0189-7
31. J.-H. Zhu, J. Deng, X.-J. Liu, J. Wang, Y.-X. Guo, and C.-B. Guo, "Prospects of robot-assisted mandibular reconstruction with fibula flap: Comparison with a computer-assisted navigation system and freehand technique." *Journal of reconstructive microsurgery*, vol. 32, pp. 661–669, Nov 2016.
32. P. Milgram and F. Kishino, "A taxonomy of mixed reality visual displays," *IEICE TRANSACTIONS on Information and Systems*, vol. 77, no. 12, pp. 1321–1329, 1994.
33. S. Nicolau, L. Soler, D. Mutter, and J. Marescaux, "Augmented reality in laparoscopic surgical oncology," *Surgical Oncology*, vol. 20, no. 3, pp. 189 – 201, 2011, special Issue: Education for Cancer Surgeons. [Online]. Available: http://www.sciencedirect.com/science/article/pii/S0960740411000521
34. R. Kikinis, S. D. Pieper, and K. G. Vosburgh, *Intraoperative Imaging and Image-Guided Therapy*. New York, NY: Springer New York, 2014, ch. 3D Slicer: A Platform for Subject-Specific Image Analysis, Visualization, and Clinical Support, pp. 277–289. [Online]. Available: https://doi.org/10.1007/978-1-4614-7657-3_19
35. O. Bimber, "Interactive rendering for projection-based augmented reality displays," Ph.D. dissertation, University of Technology Darmstadt, 9 2002.
36. C. Rossa, M. I. Keri, and M. Tavakoli, "Brachytherapy needle steering guidance using image overlay," in *Handbook of Research on Biomimetics and Biomedical Robotics*, M. Habib, Ed. Hershey, PA, USA: IGI Global, 2018, pp. 191–204. [Online]. Available: http://services.igi-global.com/resolvedoi/resolve.aspx?doi=10.4018/978-1-5225-2993-4.ch008
37. V. Ferrari, M. Carbone, S. Condino, and F. Cutolo, "Are augmented reality headsets in surgery a dead end?" *Expert Review of Medical Devices*, vol. 16, no. 12, pp. 999–1001, 2019, pMID: 31725347. [Online]. Available: https://doi.org/10.1080/17434440.2019.1693891

38. S. Condino, M. Carbone, R. Piazza, M. Ferrari, and V. Ferrari, "Perceptual limits of optical see-through visors for augmented reality guidance of manual tasks," *IEEE Transactions on Biomedical Engineering*, vol. 67, no. 2, pp. 411–419, 2020.
39. I. Howard, "Depth from motion parallax," in *Perceiving in Depth: Volume 3 Other Mechanisms of Depth Perception*. Oxford University Press, 2 2012, ch. 28.
40. R. Kooima, "Generalized perspective projection," *J. Sch. Electron. Eng. Comput. Sci*, 6 2009.
41. A. Attanasio, B. Scaglioni, E. De Momi, P. Fiorini, and P. Valdastri, "Autonomy in surgical robotics," *Annual Review of Control, Robotics, and Autonomous Systems*, vol. 4, no. 1, p. null, 2021. [Online]. Available: https://doi.org/10.1146/annurev-control-062420-090543
42. G.-Z. Yang, J. Cambias, K. Cleary, E. Daimler, J. Drake, P. E. Dupont, N. Hata, P. Kazanzides, S. Martel, R. V. Patel, V. J. Santos, and R. H. Taylor, "Medical robotics—regulatory, ethical, and legal considerations for increasing levels of autonomy," *Science Robotics*, vol. 2, no. 4, 2017. [Online]. Available: https://robotics.sciencemag.org/content/2/4/eaam8638
43. N. Hogan, "Impedance control: An approach to manipulation: Part i–theory," *J. Dyn. Sys., Meas., Control*, vol. 107, no. 1, pp. 1–7, Mar. 1985. [Online]. Available: https://doi.org/10.1115/1.3140702
44. J. Carriere, J. Fong, T. Meyer, R. Sloboda, S. Husain, N. Usmani, and M. Tavakoli, "An admittance-controlled robotic assistant for semi-autonomous breast ultrasound scanning," in *2019 International Symposium on Medical Robotics (ISMR)*, April 2019, pp. 1–7.
45. L. Cheng and M. Tavakoli, "Ultrasound image guidance and robot impedance control for beating-heart surgery," *Control Engineering Practice*, vol. 81, pp. 9 – 17, 2018. [Online]. Available: http://www.sciencedirect.com/science/article/pii/S096706611830460X
46. ——, "Switched-impedance control of surgical robots in teleoperated beating-heart surgery," *Journal of Medical Robotics Research*, vol. 03, no. 03n04, p. 1841003, 2018. [Online]. Available: https://doi.org/10.1142/S2424905X18410039
47. L. Cheng, M. Sharifi, and M. Tavakoli, "Towards robot-assisted anchor deployment in beating-heart mitral valve surgery," *The International Journal of Medical Robotics and Computer Assisted Surgery*, vol. 14, no. 3, p. e1900, 2018, e1900 RCS-17-0094.R2. [Online]. Available: https://onlinelibrary.wiley.com/doi/abs/10.1002/rcs.1900
48. M. Sharifi, H. Salarieh, S. Behzadipour, and M. Tavakoli, "Impedance control of non-linear multi-dof teleoperation systems with time delay: absolute stability," *IET Control Theory Applications*, vol. 12, no. 12, pp. 1722–1729, 2018.
49. M. Sharifi, H. Salarieh, S. Behzadipour, and M. Tavakoli, "Beating-heart robotic surgery using bilateral impedance control: Theory and experiments," *Biomedical Signal Processing and Control*, vol. 45, pp. 256 – 266, 2018. [Online]. Available: http://www.sciencedirect.com/science/article/pii/S174680941830123X
50. J. Piwowarczyk, J. Carriere, K. Adams, and M. Tavakoli, "An admittance-controlled force-scaling dexterous assistive robotic system," *Journal of Medical Robotics Research*, vol. 05, no. 01n02, p. 2041002, 2020.